RSC Advances

ROYAL SOCIETY OF CHEMISTRY

www.rsc.org/advances

Facile synthesis of flexible graphene–silver composite papers with promising electrical and thermal conductive performances

Sheng-Yun Huang [a], Kai Zhang [b], Matthew M.F. Yuen [b], Xian-Zhu Fu [a,*], Rong Sun [a,*] and Ching-Ping Wong [c, d]

[a] *Shenzhen Institutes of Advanced Technology, Chinese Academy of Sciences, Shenzhen,518055, P.R. China*

[b] *Department of Mechanical Engineering, Hong Kong University of Science and Technology, Hong Kong, P.R. China*

[c] *School of Materials Science and Engineering, Georgia Institute of Technology, Atlanta, Georgia 30332-0245, United States*

[d] *Department of Electronics Engineering, The Chinese University of Hong Kong, Hong Kong, P.R. China*

Abstract: Free-standing and flexible graphene-silver (GE-Ag) composite paper has been successfully fabricated through an evaporation of graphene oxide/$AgNO_3$ aqueous aerosol followed by a chemical reduction. The size, thickness and shape of GE-Ag paper can be tuned accordingly the Teflon substrate used. The GE-Ag paper presents the advantages of fine flexibility, high electrical conductivity (159 Ωsq^{-1}) and good thermal conductivity in the vertical direction (3.3 W/mK), which are more optimal than pure GE paper.

---

* Corresponding author. Fax: 86-755-86392151/86-755-86392299; E-mail address: xz.fu@siat.ac.cn (xz fu)
* Corresponding author. Fax: 86-755-86392158/86-755-86392299; E-mail address: rong.sun@siat.ac.cn (rong sun)

1. Introduction

Graphene (GE), a well-defined two-dimensional structure of carbon atoms, has attracted many attentions because of its unique excellent mechanical, in-plane electrical and thermal conductive performance [1-6]. For example, the thermal conductivity of GE in plane is the highest so far, more than (5.3±0.48) $\times 10^3$ W/mK [6], about 10 times higher than that of metal Ag or Cu. Unfortunately, the thermal conductivity of GE in the vertical direction is much lower than that of Ag or Cu. The GE nanosheets can be obtained by many methods, such as mechanical exfoliation [7-8], chemical vapor deposition [9-10], chemically derivate [11-12] and so on. In terms of the yield and cost, the solution phase preparation shows the most potential. However, during the solution phase preparation of GE, a challenging issue is how to avoid aggregation of GE nanosheets in the solution.

Currently Ag is usually commercially used as electrical and thermal conductive material in microelectronic and LED systems due to its high electrical and thermal conductivity [13]. But the trend is to reduce or replace Ag since it is expensive. There were lots of efforts for the work, such as: Ag coated Cu, Ag alloy, and carbon nanotube, GE, etc [14-17].

Herein, we decorated Ag nanoparticles between GE nanosheets and the GE was well dispersed in the mixture. As a result, we easily obtained freestanding GE-Ag composite paper with good thermal and electrical conductivities. The structure of the GE-Ag composite paper and effect of GE/Ag ratio were also investigated.

2. Experimental section

Materials

The natural graphite powder (carbon content: 99.85%) in the experiment was obtained from Sinopharm Chemical Reagent Co., Ltd., China. $NaBH_4$, $KMnO_4$, $NaNO_3$, concentrated H_2SO_4 (98%), concentrated HCl (36.5%), 30% H_2O_2 aqueous solutions and $AgNO_3$ with analytical purity were used as received. Deionized water was used throughout the experiments.

Synthesis of graphene oxide

Graphene oxide (GO) was prepared from natural graphite using a modified Hummers method [18]. The as-synthesized GO was suspended in water to give a brown dispersion, followed by 5 times of vacuum filtration to completely remove the residual salts and acids. Then the GO solid was dried in a vacuum oven at 60 ℃ overnight.

Preparation of graphene-silver and graphene papers

The purified GO was then dispersed in distilled water and exfoliated by ultrasonication (Branson-3500H, 1000 W) to form a 2 mg/mL suspension. Then the $AgNO_3$ solution (0.05 mol/L) was added into the GO dispersion. The obtained suspension was treated by ultrasonic treatment for 2 h and followed by stirring at room temperature for 6 h. The yellow-brown suspension was poured into Teflon plate with a diameter of 10 cm and dried at 85 ℃ for 24 h. Ag^+ ions intercalated GO paper with a diameter of 10 cm was finally obtained, which was abbreviated as GO-Ag^+ paper. GO-Ag^+ paper was soaked in sodium borohydride ethanol solution (0.35 mol/L) at 60 ℃ for 5 h and the yellow-brown paper gradually changed into black.

Meanwhile, the GE paper was prepared in the same way from GO dispersion without Ag^+ ions.

Characterization

Field emission scanning electron microscopy (SEM) images were obtained on an FEI Nova NanoSEM450 operated at 5.0 kV. X-ray diffraction (XRD) measurements were carried out by using a D/Max-3c X-ray diffractometer with Cu K (= 1.5406A°), with an operation voltage and current of 40 kV and 40 mA, respectively. Raman spectra were recorded on a Renishaw in Via Raman microscope system with 514 nm laser excitation. The mechanical properties were investigated by dynamic mechanical analyzer (DMA Q800, TA instruments).

3. Results and discussion

The GO-Ag^+ paper was easily prepared by pouring GO suspension and silver nitrate onto Teflon substrate and then placing in an oven at 85 ℃ for 24 h. In order to obtain a free-standing and flexible GE-Ag paper, sodium borohydride ethanol solution was used to reduce the composite paper, as shown in Fig. 1. Compared with water, ethanol maintains the integrity of the paper. The GE-Ag paper exhibited the properties of high electrical conductivity of 167 Ω sq^{-1}, better than that of GE paper (10^3~10^4 Ω sq^{-1}). More importantly, the presented method of an in-situ simultaneous reduction of Ag^+ ions and GO reduced the aggregation of GE nanosheets.

The surface morphology of papers has been analyzed by SEM. The SEM images of GO and GE-Ag composite papers are shown in Fig. 2. In comparison with GO paper (Fig. 2a), the surface morphology of GE-Ag composite papers were smoother (Figs.

2b-e), due to decrease of the oxygen-containing groups during reduction process. It can be found that the papers are doped by Ag nanoparticles with an average particle size from approximately 10 nm to 150 nm (Figs. 2b-f). Because the oxygen-containing groups on GO provide the chemical active centers for Ag deposition, Ag nanoparticles are separated from each other and distributed uniformly. When the mass ratio of $AgNO_3$ to GO was below 1:100, Ag nanoparticles were small and distributed well. With the increase of mass ratio, Ag nanoparticles became bigger. When the mass ratio was 1:1, agglomeration phenomenon of Ag particles were observed, as shown in Fig. 2f. Ag nanoparticles were decorating between GE layers, not only on the surface (Fig. 2e).

The Raman spectra of GO, GO-Ag^+, and GE-Ag are presented in Fig. 3. The typical features for GO paper in Raman spectra are the G line around 1590 cm^{-1} and the D line around 1325 cm^{-1}, respectively. The G line is usually assigned to the plane vibrations with E_{2g} phonon of C sp^2 atoms, while the D line is a breathing mode of k-point phonons of A_{1g} symmetry [19].The intensity ratios of the D band and G band (I_D/I_G) for GO, GO-Ag^+ and GE-Ag papers are 0.876, 0.924 and 0.787, respectively. The reduction of the peak intensity ratio in GE-Ag is due to the decreased disorder and defects in carbon atoms after the rapid chemical reduction. In addition, the peak intensities of the D band and G band in GO-Ag^+ and GE-Ag are significantly increased in comparison with GO. This indicates that the surface-enhanced Raman scattering activity results from the intense local electromagnetic fields of the Ag nanoparticles [20].

Fig. 4 shows XRD patterns of GO, GO-Ag^+ and GE-Ag. The diffraction peak is at around $2\theta=11.5^{\circ}$, corresponding to the (001) reflection of GO. According to the Bragg equation, the calculated interplanar crystal spacing of GO is from 0.335nm (pristine graphite powder) to 0.769 nm, which demonstrates that the GO has completely exfoliated. However, there are no obvious diffraction peaks of graphite oxide or graphite in the XRD patterns of GE-Ag. Recent studies have shown that, if the regular stacks of graphite oxide or graphite are destroyed, for example, by exfoliation, their diffraction peaks become weak or even disappear. It is confirmed that the regular layered structure of graphite oxide or graphite is destroyed, no matter whether the existence state of the carbon sheets is GO or GE in these composites. The peaks at $2\theta= 38.1^{\circ}$, 44.5°, 64.5°, and 77.4° can be assigned to the (111), (200), (220), and (311) crystalline planes of Ag [21], respectively, which indicate that the Ag nanoparticles are composed of pure crystalline Ag. The peaks are all ascribed to the characteristic Bragg reflections of Ag, indicating that the regular layer structures of GO or GE are disrupted Ag.

The relationship between the sheet resistance of these papers and two contributions, including mass ratio of $AgNO_3$ to GO and reduction time, has been systematically analyzed, as shown in Table 1 and Table 2,which were measured using the four-point probe detector. The electrical properties can be tuned by changing mass ratio. When the mass ratio was below 1:50, the sheet resistance decreased with the addition of $AgNO_3$; however, when the ratio was up to 1:50, the sheet resistance increased. The result shows that the mass ratio of 1:50 is turning point; the minimum sheet resistance of GE-Ag composite papers was about 359 Ωsq^{-1} (Table 1). When the reduction time was 5 h, the sheet resistance was the minimum of 159Ωsq-1, better than that of reported literature [22]. Extension of time for reduction could remove more oxygen-containing groups.

The vertical through-plane thermal conductivity of GE paper and GE-Ag (mass ratio=1:50) composite paper were investigated by TIM thermal resistance & conductivity measurement apparatus (LW-9389，Fig 5). It is found that the thermal conductivity of papers decreased with thickness increasing (Fig.6). This result was attributed to the relationship between thickness of papers and reduction degree. The GO-Ag^+ papers reduced completely show a higher thermal property than that reduced partially because of the presence of effective reduction depth. GE-Ag composite papers afford a maximum thermal conductivity of 3.3 W/mK (25 μm) and 2.0 W/mK (55 μm), which is significantly higher than that of GE papers 2.4 W/mK (25 μm) and 1.5 W/mK (55 μm). Incorporating Ag nanoparticles between GE sheets will hinder restacking and provide conductive paths between sheets.

The mechanical properties of GO papers and GE-Ag papers were investigated by a tensile test, as shown in Figure 7. Compared with GO papers, the GE-Ag papers exhibit enhanced Young's modulus with a simultaneous slightly decrease in tensile strength. The values are much larger than that of commercial flexible graphite paper (about 10Mpa).[23]

4. Conclusions

Free-standing and flexible GE-Ag composite papers with uniformly layered structures were fabricated by a facile reduction method. The existing of Ag nanoparticles inhibits the GE sheets from restacking and aggregating, which can reserve the outstanding performance of GE. In comparison with GE papers, the surface resistance of GE-Ag composite papers decreased from 10^3~10^4 to 159 Ωsq^{-1}, and the thermal conductivity in vertical direction with the enhancement more than 35.2%. The Ag nanoparticles play a crucial role in improving properties of the papers because of reducing the surface reflectance and providing conductive paths. The mechanical properties of GE-Ag papers are supposed to satisfy the requirement of application. The convenient and large-scale method presented here provides an efficient and promising way to produce high-performance and low-cost GE-Ag composite paper with high electrical and thermal conductivities.

Acknowledgements

This work was financially supported by the National Natural Science Foundation of China (No. 21203236), Guangdong and Shenzhen Innovative Research Team Program (No.2011D052, KYPT20121228160843692), the Shenzhen Electronic Packaging Materials Engineering Laboratory (2012-372).

References

1 Novoselov KS, Geim AK, Morozov SV, Jiang D, Zhang Y, Dubonos SV, et al. Science 2004; 306(5696):666–9.

2 Novoselov KS, Geim AK, Morozov SV, Jiang D, Katsnelson MI, Grigorieva IV, et al. Nature 2005; 438:197–200.

3 Geim AK, Novoselov KS. Nat Mater 2007; 6(3):183–91.

4 QZ Liang, XX Yao, W Wang, Y Liu, and CP Wong. ACS Nano 2011; 5(3):2392-401.

5 Raza M, Westwood A, Brown A, Hondow N, Stirling C. Carbon 2011; 49:4269-79.

6 Balandin AA, Ghosh S, Bao WZ, Calizo I, Teweldebrhan D, Miao F, et al. Nano Lett 2008; 8(3):902–7.

7 Li XL, Zhang GY, Bai XD, Sun XM, Wang XR, Wang EG, et al. Nat Nanotechnol 2008; 3:538-42.

8 Michael JM, Li JL, Adamson DH, Schniepp HC, Abdala AA, Liu J, et al. Chem Mater,2007; 19:4396-404.

9 Somani PR, Somani SP, Umeno M. Chem Phys Lett 2006; 430:56-9.

10 Kim KS, Zhao Y, Jang H, Lee SY, Kim JM, Kim KS, et al. Nature 2009; 457:706-10.

11 Stankovich S, Dikin DA, Dommett GHB, Kohlhaas KM, Zimney EJ, Stach EA, et al. Nature 2006; 442:282-6.

12 Gomez-Navarro C, Weitz RT, Bittner AM, Scolari M, Mews A, Burghard M, et al. Nano Lett 2007; 7(11):3499-503.

13 Solomon SD, Bahadory M, Jeyarajasingam AV, Rutkowsky SA, Boritz B. J Chem Educ 2007; 84(2):322-5.

14 Zhang RW, Lin W, Lawrence K, Wong CP. Int J Adhes Adhes 2010; 30:403-7.

15 Jang SH, Lim JH, Kim JH, Ji BK, Joo J, Nah W, et al. IEEE Trans on Appl Supercond 2003; 13(2):2956-9.

16 Yang GW, Gao GY, Wang C, Xu CL, Li HL. Carbon 2008; 46(5):747-52.

17 Xiang J, Drazal LT. Carbon 2011; 49:773-8.

18 Hummers WS, Offeman RE. J Am Chem Soc 1958; 80(6):1339.

19 Kudin KN, Ozbas B, Schniepp HC, Prud'homme RK, Aksay IA, Car R. Nano Lett 2008; 8(1):36–41.

20 Zhou L, Gu HM, Wang C, Zhang JL, Lv M, He RY. Colloids and Surfaces A: Physicochem Eng Aspects 2013; 430:103-9.

21 Baby TT, Ramaprabhu S. J Mater Chem 2011; 21:9702-9.

22 RG Gao, NT Hu, Z Yang, QR Zhu, et al. Nanoscale Reasearch Letters 2013; 8:32-9.

23 XH Wei, L Liu, JX Zhang, JL Shi, QG Guo. J Mater Sci 2010; 45:2449-55.

Figure Captions

Fig. 1 Digital camera images of the as GO-Ag^+ and GE-Ag paper.

Fig. 2 SEM images of surface morphologies of different papers. (a) GO paper, (b-f) GE-Ag composite papers (mass ratio of $AgNO_3$: GO is from 1:200 to 1:1).

Fig. 3 Raman spectra of GO, GO-Ag^+, GE-Ag.

Fig.4 XRD patterns of GO and composites. (a) GO, (b) GO-Ag^+, (c) GE-Ag.

Table 1 The electrical properties of the GE-Ag paper for different mass ratio (Reduction time: 4h).

Table 2 The electrical properties of the GE-Ag paper for different reduction Time (The mass ratio is 1:50).

Fig.5 The schematic diagram thermal interface material testing principle.

Fig.6 Through-plane thermal conductivity of GE paper and GE-Ag composite paper.

Fig.7 Mechanical properties of GO paper and GE-Ag papers for different mass ratio: (a)Young's modulus; (b)tensile strength.

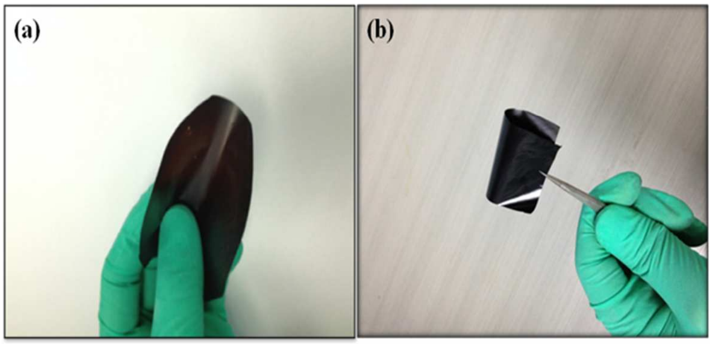

Fig. 1 Digital camera images of the as GO-Ag$^+$ and GE-Ag paper.

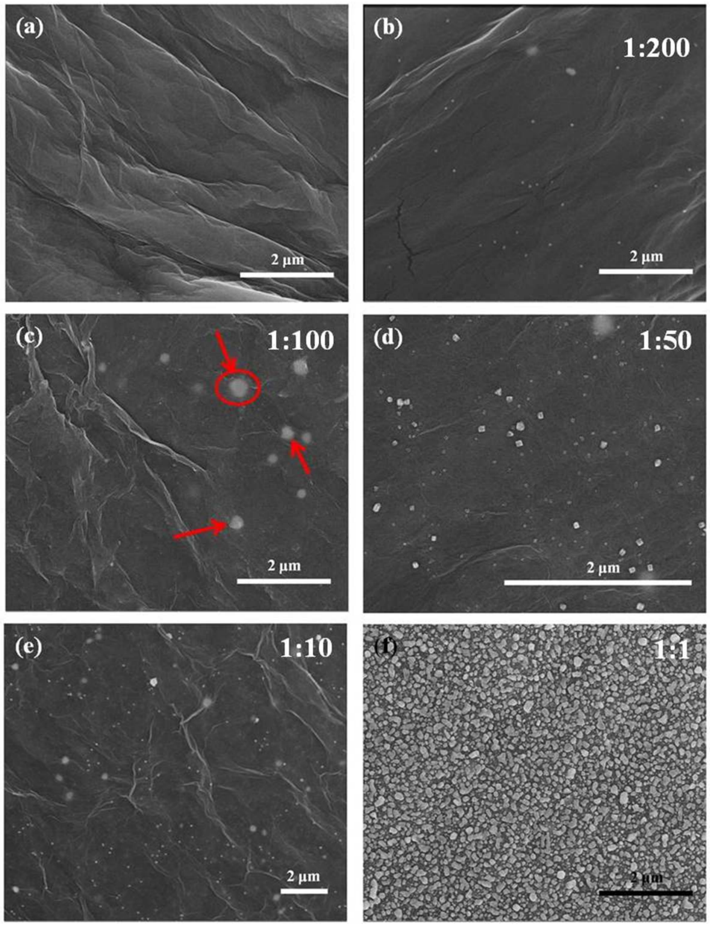

Fig. 2 SEM images of surface morphologies of different papers. (a) GO paper, (b-f) GE-Ag composite papers (mass ratio of $AgNO_3$: GO is from is from 1:200 to 1:1).

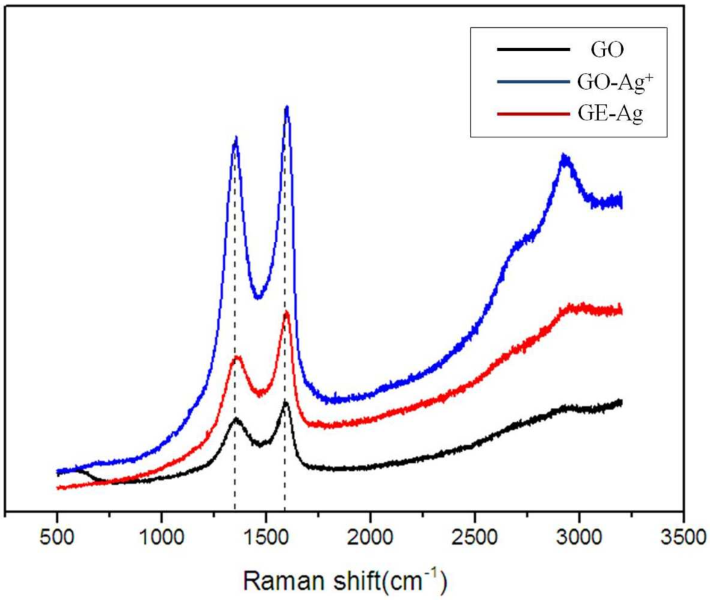

Fig. 3 Raman spectra of GO, GO-Ag$^+$, GE-Ag.

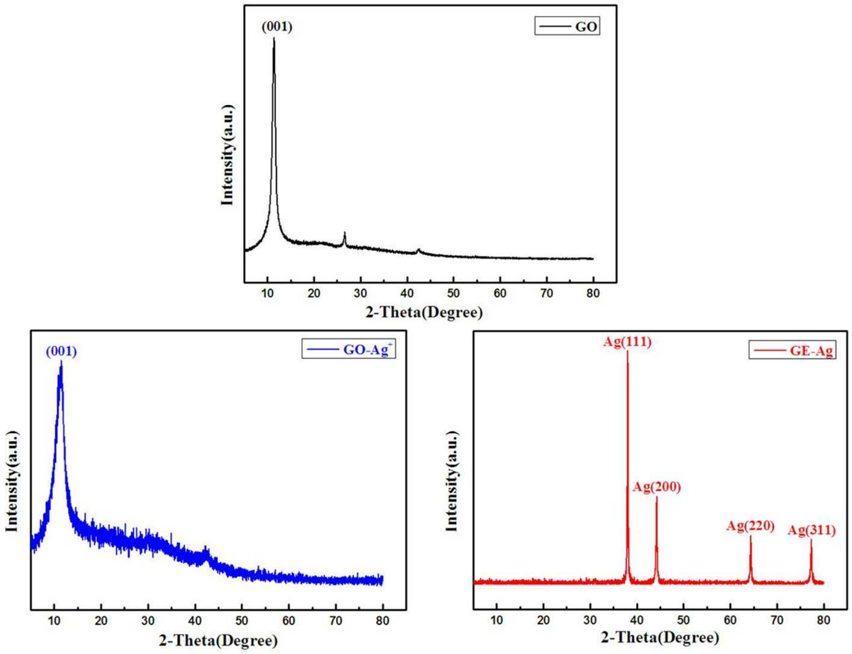

Fig.4 XRD patterns of GO and composites. (a) GO, (b) GO-Ag^+, (c) GE-Ag.

Table 1 The electrical properties of the GE-Ag paper for different mass ratio (Reduction time: 4h).

Mass Ratio	**1:200**	**1:100**	**1:50**	**1:10**	**1:1**
Sheet resistance (Ωsq^{-1})	9564	5679	359	1700	6218

Table 2 The electrical properties of the GE-Ag paper for different reduction Time (The mass ratio is 1:50).

Reduction Time	**1h**	**2h**	**5h**
Sheet resistance (Ωsq^{-1})	7383	3456	159

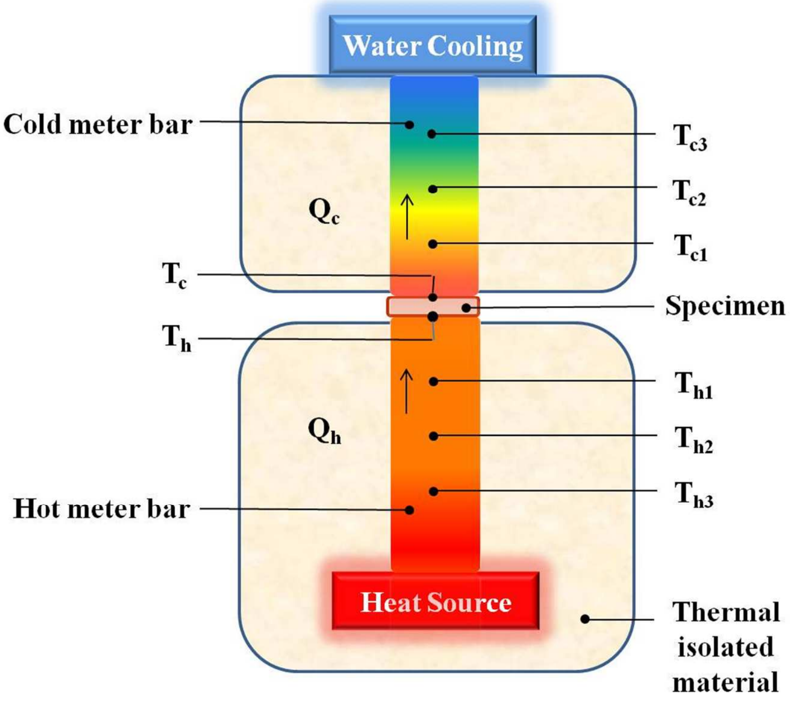

Fig.5 The schematic diagram thermal interface material testing principle.

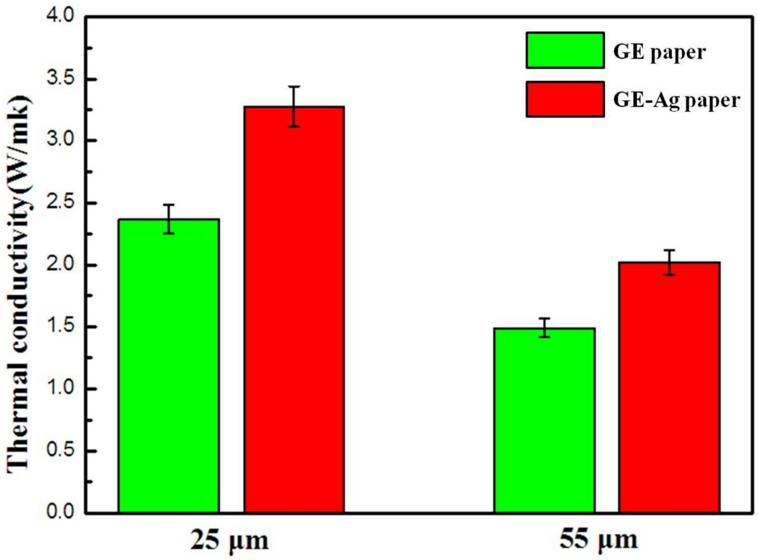

Fig.6 Through-plane thermal conductivity of GE paper and GE-Ag composite paper.

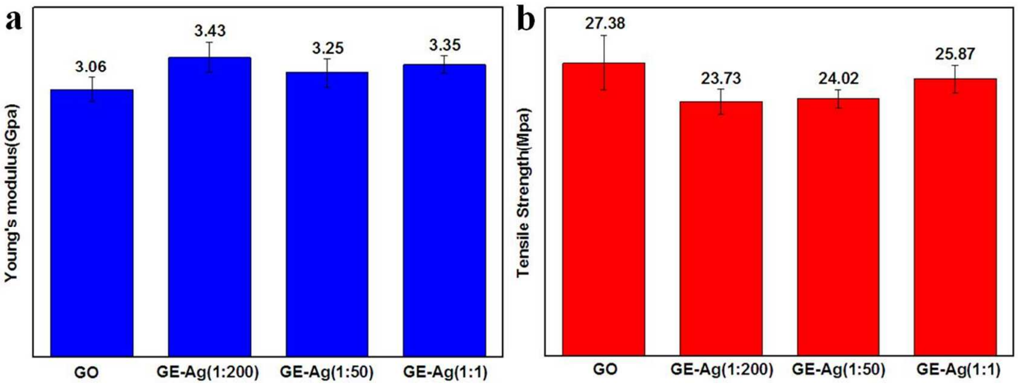

Fig.7 Mechanical properties of GO paper and GE-Ag papers for different mass ratio: (a) Young's modulus, (b)tensile strength.